UDK 669.018:621.791.725
Original scientific article/Izvirni znanstveni članek

ISSN 1580-2949
Mater. Tehnol.

ADDITIVE MANUFACTURING OF ARCHITECTED INCONEL 718 STRUCTURES: EXPLORING THE STRENGTH AND FAILURE OF LATTICE STRUCTURES

ARHITEKTURA STRUKTUR SUPERZLITINE INCONEL 718 IZDELANIH Z DODAJALNO TEHNOLOGIJO; UGOTAVLJANJE TRDNOSTI IN NAPAK V STRUKTURNIH MREŽAH

Sami Westman[1*], Ahmed W. Abdelghany[2,3*], Mahmoud Khedr[1,2,4], Lari Rajala[1], Ilkka Poutiainen[1], Antti Järvenpää[1,2]

[1]Laser Processing and Additive Manufacturing, Mechanical Engineering Department, School of Energy Systems, Lappeenranta-Lahti University of Technology (LUT), P.O. Box 20, FI-53851 Lappeenranta, Finland
[2]Future Manufacturing Technologies (FMT), Kerttu Saalasti Institute, University of Oulu, Nivala 85500, Finland
[3]Design and Production Engineering Dept., Faculty of Engineering, Ain Shams University, Cairo 11535, Egypt
[4]Mechanical Engineering Department, Faculty of Engineering at Shoubra, Benha University, Cairo 11629, Egypt

Prejem rokopisa – received: 2025-09-24; sprejem za objavo – accepted for publication: 2026-02-19

doi:10.17222/mit.2025.1578

This study investigates the mechanical performance and failure behaviour of additively manufactured Inconel 718 (IN718) lattice structures fabricated via laser powder bed fusion (PBF-LB). Five distinct unit-cell topologies were evaluated: three triply periodic minimal surfaces (TPMSs), namely Schoen gyroid (SG), Schwarz diamond (SD), and Schwarz primitive (SP), and two beam-based strut lattices with body-centred cubic (BCC) and beam diamond (BD) unit cells. All specimens were fabricated on an EOS M290 system with a controlled infill density of approximately 18–20 % and subjected to the manufacturer-recommended solution and ageing heat treatment for IN718. Monotonic tensile tests were performed to quantify the ultimate tensile strength (UTS) and to evaluate topology-dependent failure mechanisms. The results reveal a pronounced architectural influence on tensile performance, with TPMS lattices consistently outperforming beam-based designs. Among all configurations, the SD lattice achieved the highest UTS, reaching approximately 817 MPa, whereas the BCC lattice exhibited the lowest UTS, 315 MPa. Fractographic analysis showed that beam-based structures failed predominantly at strut–node intersections, while TPMS lattices displayed micro-void coalescence with local shear facets, indicative of distributed ductile tearing. Overall, the results indicate that TPMS geometries exhibit superior tensile performance compared with conventional beam lattices in static load-bearing applications.

Keywords: additive manufacturing, laser powder bed fusion, lattice structures, Inconel 718

V članku avtorji predstavljajo študijo mehanskih lastnosti in obnašanje izbranega materiala (superzlitine Inconel 718 tipa IN718) zaradi odpovedi posameznih mrežnih struktur. Različne arhitekture superzlitine so bile izdelane z dodajalno tehnologijo laserskega taljenja in medsebojnega sintranja posameznih plasti kovinskega prahu (PBF-LB; angl.: Laser Powder Bed Fusion). Avtorji so izdelali in ocenili pet različnih topologij enotnih celic: tri-trikrat periodične minimalne površine (TPMS), in sicer Shoenov giroid (SG; Schoen Gyroid), Schwarzov diamant (SD; Schwarz Diamond) in Schwarzova osnovna kocka (SP; Schwarz Primitive), ter dve mreži na osnovi nosilcev s kubičnimi enotnimi celicami, ploskovno centrirano kubično (BCC; angl.: body-centred cubic) in diamantno (BD; angl.: beam dimond). Vse vzorce so avtorji izdelali na laserskem sistemu podjetja EOS M290 z nadzorovano gostoto polnjenja (približno 18–20 %). Izdelani vzorci (natezni preizkušanci) so bili nato še naknadno toplotno obdelani z raztopnim žarjenjem ter staranjem po priporočilih proizvajalca za superzlitino IN718. Sledili so natezni preskusi za določitev končne natezne trdnosti (UTS) in oceno mehanizmov odpovedi, odvisnih od topologije. Rezultati preizkusov so pokazali izrazit vpliv arhitekture na natezno trdnost, pri čemer so TPMS mreže dosledno prekašale zasnove na osnovi nosilcev. Med vsemi konfiguracijami so pri SD mreži dosegli najvišjo natezno trdnost (približno 817 MPa), medtem ko je BCC mreža imela najnižjo natezno trdnost (315 MPa). Analiza prelomov je pokazala, da so se strukture na osnovi nosilcev porušile predvsem na presečiščih opornikov in vozlišč, medtem ko so TPMS mreže pokazale koalescenco (mehanizem združevanja) mikropraznin z lokalnimi strižnimi fasetami (stopnicami), kar kaže na porazdeljeno duktilno trganje. Na splošno rezultati kažejo, da imajo TPMS geometrije boljšo natezno trdnost v primerjavi s konvencionalnimi mrežami nosilcev za statične nosilne aplikacije.

Ključne besede: izdelava mrežnih struktur z dodajalno tehnologijo, postopek laserskega taljenja in sintranja posameznih plasti kovinskega prahu, mrežne strukture, superzlitina Inconel 718

1 INTRODUCTION

Laser powder bed fusion (PBF-LB) is an additive manufacturing (AM) technique, in which a laser beam selectively fuses regions of a metal powder bed in successive layers to build three-dimensional parts.[1,2] This process allows the manufacturing of complicated geometries without additional processes, decoupling complexity from fabrication time. Such geometric freedom enables mass reduction via architected lattice structures, replacing solid volumes with controlled porosity while tailoring mechanical performance.[2]

*Corresponding author's e-mail:
sami.westman@lut.fi (Sami Westman)

Lattice architectures fall broadly into strut-based (beam) and sheet-based triply periodic minimal surface (TPMS) categories. The mechanical properties of lattice structures, such as stiffness, strength, and energy absorption, scale with relative density according to power-law relationships derived from the cellular solids theory (Gibson & Ashby).[3] TPMS designs (e.g., Schoen Gyroid, SG; Schwarz Diamond, SD; Schwarz Primitive, SP) offer smoothly curved, continuous surfaces that suppress stress concentrations, yield higher specific strength, and facilitate transport or multifunctionality, unlike node-dominated beams.[4,5] Recent optimisation studies further refine wall thickness or grading to shift load distribution and improve performance at fixed mass.[4] Yet, direct tensile comparisons of mixed TPMS and beam-based lattices in the same alloy and density remain limited, as most literature emphasises compression behaviour or single-topology studies.[5]

Inconel 718 (IN718), a nickel-based superalloy, is widely employed in high-temperature structural components owing to its precipitation-hardening capability, corrosion resistance, and weldability.[6] After solution treatment and ageing, IN718 exhibits high tensile strength and ductility – properties that can be retained or partially modified in lattice architectures.[7,8] Microstructural analyses of PBF-LB IN718 show $\gamma/\gamma'/\gamma''$ phases and partial recrystallisation depending on heat treatment, influencing yield behaviour and strain capacity.[9] Several studies have investigated the mechanical behaviour of additively manufactured lattice structures; however, most reports focus either on strut-based lattices or on TPMS architectures, often under compressive loading. Studies comparing TPMS and strut-based lattices have consistently shown superior strength and energy absorption for TPMS geometries, particularly diamond-type structures, but these investigations are largely limited to compression and/or non-nickel alloys.[10,11] More recently, Ferrarotti et al. examined INC718 lattices fabricated by PBF-LB, focusing on the microstructure and compressive behaviour of multiple lattice topologies.[12]

Consequently, a clear gap remains in the literature regarding systematic tensile performance data for INC718 lattices across different architectural configurations, which is essential for a reliable design of load-bearing structural components. This gap is particularly critical given the strong potential of IN718 lattice structures for lightweight, high-temperature applications such as aerospace components and compact heat exchangers, where high specific strength is required. Moreover, generating robust, transferable mechanical data for lattice structures requires larger, more controlled datasets than for bulk materials. Due to their small feature sizes and high surface-to-volume ratios, lattice architectures are highly sensitive to variations in manufacturing conditions.

The present study addresses these challenges by providing a controlled tensile comparison of TPMS and beam-based IN718 lattices at matched volume fraction, thereby isolating the effect of architecture on tensile strength and failure behaviour. Five IN718 lattice types were fabricated by PBF-LB and subjected to supplier-recommended heat treatment. The investigated architectures comprise three TPMS geometries (SG, SD, SP) and two beam lattices (BCC and BD). Mechanical performance is assessed through monotonic tensile testing, and fracture surfaces are analysed by scanning electron microscopy (SEM) to correlate failure mechanisms to architectural topology.

2 EXPERIMENTAL PART

2.1 Materials and lattice design

Five distinct unit-cell topologies were investigated in this study: three TPMS designs (SG, SD, and SP) and two beam-based lattices (BCC and BD). The design requirements included a uniform unit-cell geometry within the tensile gauge region and a target volume fraction of approximately 18–20 %. TPMS lattices employed a wall thickness of 1.0 mm, whereas beam lattices used a strut thickness of 2.0 mm to achieve comparable relative density. The lattice parameters listed in **Table 1** were selected to ensure similar material usage across all architectures. Unit-cell dimensions were adjusted to ensure that the gauge cross-section consisted exclusively of complete cells, thereby avoiding truncated units that may introduce geometric discontinuities and reduce structural efficiency. Uniform cell geometry was maintained throughout the gauge region to preserve consistent strut orientation and load transfer. Several preliminary design trials were conducted to confirm manufacturability and to ensure that fractures consistently occurred within the lattice gauge section. The minimal cross-sectional area was determined from a horizontal section through the gauge region. The resulting geometrical parameters are summarised in **Table 1.**

Table 1: Geometry data of the AM IN718 lattice specimens used in tensile testing

Lattice type	Cell size, mm	Thickness (t), mm	Volume fraction, %	Minimal cross-sectional area, mm^2
Schoen gyroid (SG)	10 × 10 × 10	1.0	19.5	51.1
Schwarz diamond (SD)	12.5 × 12.5 × 12.5	1.0	18.5	45.8
Schwarz primitive (SP)	17.5 × 17.5 × 17.5	1.0	18.7	34.5
Body centred cubic (BCC)	10 × 10 × 10	2.0	18.2	29.1
Beam diamond (BD)	10 × 10 × 10	2.0	17.8	45.9

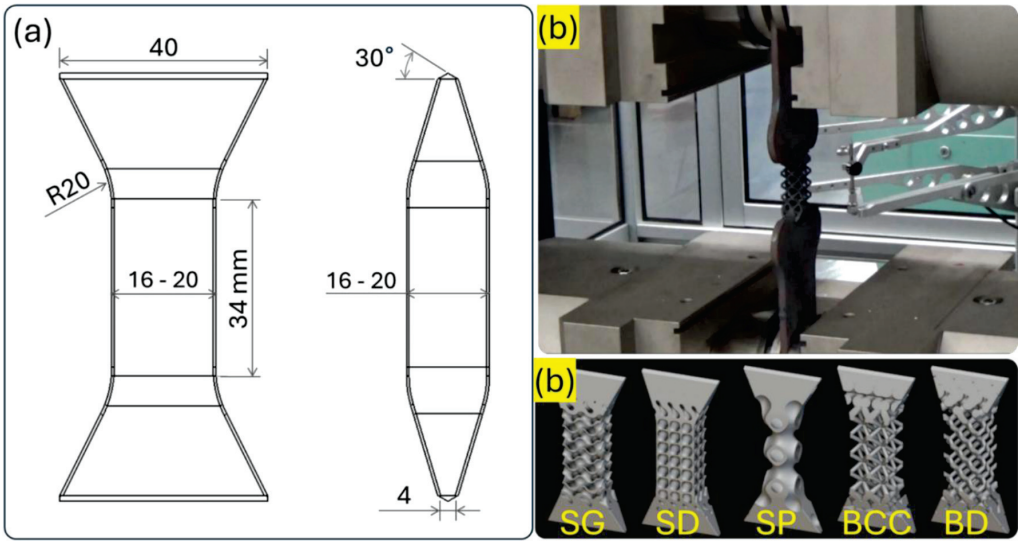

Figure 1: Tensile specimen and test set-up: a) geometry of the bow-tie coupon used for lattice tensile tests, b) universal testing machine configuration, and c) lattice topologies examined

2.2 Additive manufacturing and testing

All specimens were additively manufactured by PBF-LB on an EOS M290 using EOS NickelAlloy IN718 powder and the EOS-validated IN718 parameter set (laser power–scan speed–hatch spacing combination) optimised for high density and stable processing. The powder utilized for the print was a pre-alloyed IN718 (gas-atomized, spherical particles), with a particle size distribution of approximately 20–63 μm. The nominal powder's chemical composition was Ni ≈50–55 *w*/%, Cr ≈17–21 *w*/%, Nb ≈4.8–5.5 *w*/%, Mo ≈2.8–3.3 *w*/%, Ti ≈0.7–1.1 *w*/%, Al ≈0.2–0.8 *w*/%, Fe balance, and minor elements within the limits specified by the supplier.[13]

To confirm the bulk additively manufactured material properties, standard tensile coupons were fabricated in the same build direction as the lattice specimens, in accordance with SFS-EN ISO 6892-1b. The lattice tensile coupons were built horizontally on the build plate. After removal from the substrate, the lattice sections were welded to slotted 6 mm-thick steel plates to facilitate gripping during testing. The final specimen geometry and test configuration are shown in **Figure 1**. Within the tensile gauge region, the lattice cell size was held constant and then gradually increased toward the ends to form fully solid tabs. Post-processing followed the EOS-recommended heat treatment for Inconel 718: solution annealing at 954 °C for 1 h, air-cooled to room temperature; ageing at 718 °C for 8 h; furnace cooling to 621 °C; and holding until a total ageing time of 18 h was reached.[13]

Monotonic tensile tests were conducted using a Galdabini Quasar 600 universal testing machine. As no standard currently exists for tensile testing of lattice structures, lattice specimens were specifically designed to promote fracture within the lattice gauge region. All tests were performed under crosshead displacement control at a nominal strain rate of 0.05 min^{-1} and at room temperature (21 °C). Due to the complex and open geometry of the lattice specimens, the use of a conventional extensometer was infeasible. Consequently, specimen elongation was measured from the crosshead displacement. The minimal cross-sectional area listed in **Table 1** was used for stress normalisation. Fracture surfaces were examined using a JEOL JSM-7900F field-emission scanning electron microscope (FESEM) to identify dimpled regions, cleavage or shear facets, and process-related defects.

3 RESULTS AND DISCUSSION

Figure 2a presents the engineering stress–strain response of the solid IN718 verification coupons, confirming the build quality and heat treatment. The average ultimate tensile strength (UTS) was ≈1389 MPa, and the yield strength (YS) was č1191 MPa, modestly below the supplier's reference values (UTS 1505 MPa; YS 1240 MPa). The differences (≈8 % in UTS and ≈4 % in yield) are small and are probably attributable to powder history and/or minor variations in thermal exposure or cooling rate during heat treatment. Moreover, **Figure 2a** shows the full tensile behaviour of the lattice specimens, clearly demonstrating markedly lower elongation compared with the solid baseline and revealing distinct peak-and-drop signatures for each topology. In this view, SD reaches the highest peak stress before a sharp loss of load, SP shows a more progressive stepwise decline, and the BCC lattices exhibit earlier loss of ductility.

Across the five lattice topologies, SD exhibited the highest UTS (≈817 MPa), while BCC showed the lowest value (≈325 MPa). Notably, SD and BD have nearly identical minimum cross-sectional areas (≈45.8 vs 45.9 mm^2), yet SD noticeably outperforms BD. This re-

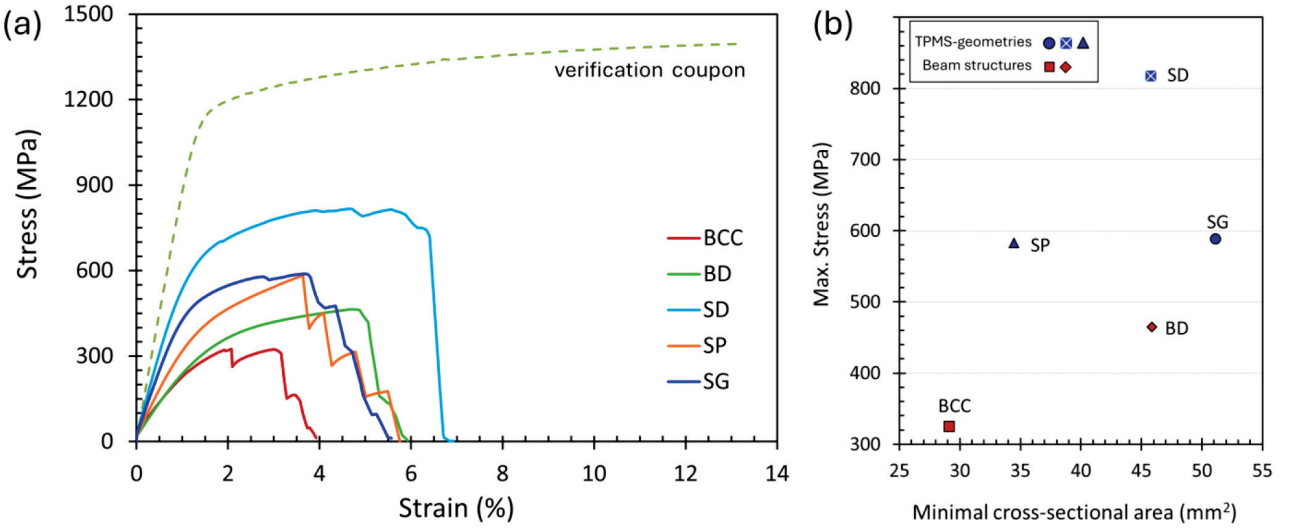

Figure 2: Tensile behaviour of AM IN718 lattices: a) engineering stress–strain curves, b) scatter of maximum stress vs minimal cross-sectional area

flects the fundamental architectural advantage of TPMSs, where smooth, continuous surfaces distribute load and suppress local stress concentrations, whereas beam lattices concentrate stress at strut–node junctions, promoting early crack initiation and limiting peak stress.[4] This indicates that the primitive topology leverages its material more effectively in the tensile direction, resulting in greater specific strength than the gyroid despite using less cross-sectional area. Prior studies have observed that the diamond-type TPMS yields the highest strength among such minimal surfaces, while the primitive type can also outperform the gyroid under comparable conditions.[5] Another informative comparison is SP versus SG. Despite SP having a smaller minimal area (34.5 vs 51.1 mm^2), its maximum stress is comparable to SG (≈583 vs ≈588 MPa), indicating higher tensile efficiency of the primitive topology under these test conditions. Overall, TPMS lattices (SD, SG, SP) outperformed beam lattices (BD, BCC) at similar relative densities, and SD emerged as the top performer among all designs. The lattice stress–strain curves also reveal distinct failure signatures. SD shows a well-defined peak followed by an abrupt load drop, consistent with a more global failure of a continuous shell network. However, SP and BCC tend to fail progressively, segment by segment, in line with their topology and lower cross-sectional area.

Figure 3 shows representative SEM fracture surfaces for the five lattices. The TPMS lattices (SG, SD, SP) ex-

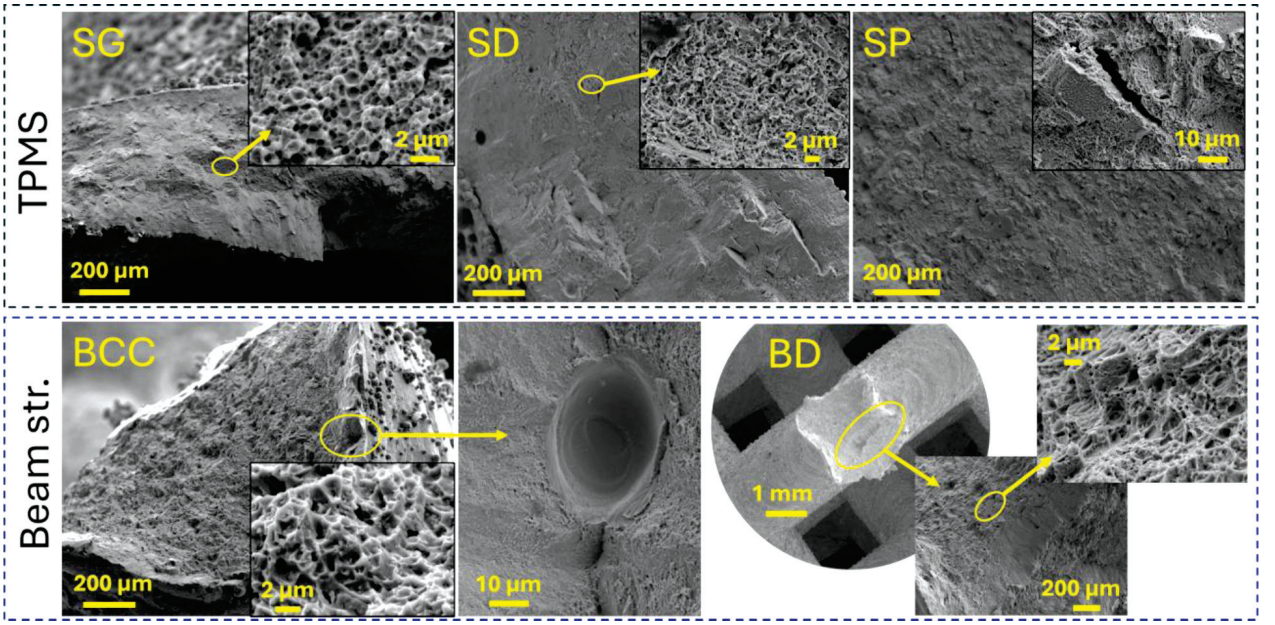

Figure 3: SEM fracture surfaces after tensile testing of AM IN718 lattices: SG, SD, SP (top) and BCC, BD (bottom). Insets highlight local features.

hibit distributed micro-void coalescence with shear facets, reflecting ductile fracture and more uniform stress fields. In contrast, the beam lattices (BCC, BD) fractured at strut–node junctions, where stress concentration and local defects promoted early accumulation of damage and instability. These topology-dependent damage sites agree with established observations that TPMSs reduce stress concentrations relative to node-dominated beam networks.[10]

The tensile curves (**Figure 2a**) follow directly from these micromechanisms. SD shows a pronounced peak and a sudden drop in load in a continuous shell network, whereas SP exhibits a stepwise post-peak descent, consistent with progressive crack advance across thinner struts. All lattices peak below the solid-coupon baseline (UTS ≈ 1389 MPa; YS ≈ 1191 MPa), which is expected for architected media with indirect load paths, reduced effective area, and local bending induced by geometric variation, specifically for strut networks, explaining the group separation between beam and TPMS designs. The damage initiation sites (plane vs nodes) govern the post-yield trajectory and the peak stress. TPMSs minimise stress concentration and postpone instability, yielding the hierarchy SD > SG ≈ SP > BD > BCC observed in tension.[9]

The enhanced tensile performance of TPMS lattices observed in this study can be attributed to their continuous shell-based architecture, which promotes smoother stress fields and reduces stress concentrations compared to beam lattices. Studies of stainless steel and Ti-6Al-4V lattices have shown that TPMS geometries distribute stresses more uniformly than BCC-type lattices.[10,11] The studies have shown that strut-based lattices fail preferentially at node junctions due to high local triaxiality and bending-dominated deformation. This interpretation is consistent with the fractography results of the present work, in which TPMS specimens exhibited distributed micro-void coalescence and shear features, whereas beam lattices showed fracture initiation at strut–node intersections. Although direct tensile data for IN718 TPMS lattices are limited, it has been reported that the compressive strength of IN718 lattices is strongly governed by architecture rather than by microstructural differences, supporting the present findings.[12]

4 CONCLUSIONS

The present study demonstrates that the tensile response of PBF-LB-processed IN718 lattice structures is governed primarily by architectural topology rather than by minimal cross-sectional area alone. At a controlled relative density of approximately 18–20 %, triply periodic minimal surface (TPMS) lattices (SG, SD, and SP) consistently exhibited higher ultimate tensile strength than the beam-based lattices (BD and BCC). Among all configurations, the SD lattice exhibited the highest tensile strength (≈817 MPa), approximately 59 % of the UTS of solid IN718, while using only a fraction of the material, highlighting its high specific strength, whereas the BCC lattice showed the lowest value, approximately 325 MPa. Notably, despite nearly identical minimum cross-sectional areas (≈46 mm^2), the SD lattice significantly outperformed the BD lattice, highlighting the superior load-carrying efficiency of a continuous structure over node-dominated struts. Furthermore, the SP lattice attained a tensile strength comparable to that of the SG despite a smaller minimal cross-section, indicating a higher tensile efficiency for the primitive topology under the investigated conditions. Fractographic SEM analysis supports these observations, as TPMS lattices exhibited distributed micro-void coalescence with local shear facets, whereas beam lattices failed predominantly at strut–node junctions, explaining the observed differences in post-yield behaviour and the overall strength ranking (SD > SG ≈ SP > BD > BCC).

Acknowledgment

The authors gratefully acknowledge the Laser Laboratory at LUT University and the Future Manufacturing Technologies (FMT) group at the University of Oulu for providing the research facilities. This work was also supported by the project Rakenninnovaatioden Digitaalinen Kehittäminen (RAKEDIGI), project code A81702.

5 REFERENCES

[1] H. Hosseinlou, M. Shakeri, A. W. Abdelghany, M. Jaskari, A. Järvenpää, A. Hamada, Tailoring microstructure and mechanical properties of additively manufactured H13 tool Steel: Influence of build orientation and tempering treatments, Materials Science and Engineering: A, 942 (**2025**), 148708, doi:10.1016/j.msea.2025.148708

[2] S. F. Nabavi, A. Farshidianfar, H. Dalir, Comprehensive review: Advancements in modeling geometrical and mechanical characteristics of laser powder bed fusion process, Optics & Laser Technology, 180 (**2025**), 111480, doi:10.1016/j.optlastec.2024.111480

[3] G. Epasto, G. Palomba, D. D'Andrea, E. Guglielmino, S. Di Bella, F. Traina, Ti-6Al-4V ELI microlattice structures manufactured by electron beam melting: Effect of unit cell dimensions and morphology on mechanical behaviour, Materials Science and Engineering: A, 753 (**2019**), 31–41, doi:10.1016/j.msea.2019.03.014

[4] J. Zhu, S. Zou, Y. Mu, J. Wang, Y. Jin, Additively Manufactured Scaffolds with Optimized Thickness Based on Triply Periodic Minimal Surface, Materials, 15 (**2022**), 7084, doi:10.3390/ma15207084

[5] Y. Li, D. Jiang, R. Zhao, X. Wang, L. Wang, L.-C. Zhang, High Mechanical Performance of Lattice Structures Fabricated by Additive Manufacturing, Metals, 14 (**2024**), 1165, doi:10.3390/met14101165

[6] A. Hilaire, E. Andrieu, X. Wu, High-temperature mechanical properties of alloy 718 produced by laser powder bed fusion with different processing parameters, Additive Manufacturing, 26 (**2019**), 147–160, doi:10.1016/j.addma.2019.01.012

[7] X. Qi, X. Liang, J. Wang, H. Zhang, X. Wang, Z. Liu, Microstructure tailoring in laser powder bed fusion (L-PBF): Strategies, challenges, and future outlooks, Journal of Alloys and Compounds, 970 (**2024**), 172564, doi:10.1016/j.jallcom.2023.172564

[8] N. K. Adomako, N. Haghdadi, S. Primig, Electron and laser-based additive manufacturing of Ni-based superalloys: A review of heterogeneities in microstructure and mechanical properties, Mate-

rials & Design, 223 (**2022**), 111245, doi:10.1016/j.matdes.2022.111245

[9] A. Santoni, M. Cabibbo, M. Mandolini, et al., Laser Powder Bed Fusion Inconel 718 Lattice Structures: From Process Simulation to Microstructural and Mechanical Characterizations, Metals and Materials International, (**2025**), doi:10.1007/s12540-025-01963-2

[10] B. Sokollu, O. Gulcan, E. I. Konukseven, Mechanical properties comparison of strut-based and triply periodic minimal surface lattice structures produced by electron beam melting, Additive Manufacturing, 60 (**2022**), 103199, doi:10.1016/j.addma.2022.103199

[11] L. Zhang, S. Feih, S. Daynes, S. Chang, M. Y. Wang, J. Wei, W. F. Lu, Energy absorption characteristics of metallic triply periodic minimal surface sheet structures under compressive loading, Additive Manufacturing, 23 (**2018**), 505–515, doi:10.1016/j.addma.2018.08.007

[12] A. Ferrarotti, F. Giuffrida, E. Sharghivand, G. Mussino, M. Vedani, M. Baricco, A. Castellero, Mechanical and microstructural properties of IN718 additively manufactured lattice structures, Materials Science and Engineering: A, 919 (**2025**), 147491, doi:10.1016/j.msea.2024.147491

[13] EOS NickelAlloy IN718 Material Data Sheet, online: https://www.eos.info/var/assets/05-datasheet-images/Assets_MDS_Metal/EOS_NickelAlloy_IN718/Material_DataSheet_EOS_NickelAlloy_IN718_en.pdf?v=3